Water Research 146 (2018) 275–287

Contents lists available at ScienceDirect

Water Research

journal homepage: www.elsevier.com/locate/watres

Inhibitory effects of ammonia on syntrophic propionate oxidation in anaerobic digester sludge

Chen Zhang [a, b], Quan Yuan [c], Yahai Lu [b, *]

[a] State Key Laboratory of Biochemical Engineering, Institute of Process Engineering, Chinese Academy of Sciences, Beijing, 100190, China
[b] College of Urban and Environmental Sciences, Peking University, Beijing, 100871, China
[c] State Key Laboratory of Environmental Geochemistry, Institute of Geochemistry, Chinese Academy of Sciences, Guiyang, 550081, China

ARTICLE INFO

Article history:
Received 15 June 2018
Received in revised form
30 August 2018
Accepted 21 September 2018
Available online 27 September 2018

Keywords:
Syntrophic propionate oxidation
Methanogenesis
Ammonia stress
Anaerobic digester
Stable isotope probe

ABSTRACT

Syntrophic propionate oxidation (SPO) coupled with methanogenesis is often inhibited under high ammonium concentrations in anaerobic digesters. However, the inhibitory mechanism remains poorly understood. We conducted two independent laboratory experiments with a swine manure digester sludge. In experiment I, RNA-based stable isotope probing (SIP) was applied to determine the active players of both bacteria and methanogens involved in SPO under different ammonium concentrations (0, 3 and 7 g NH_4^+–N L^{-1}). In experiment II, the dynamics of the bacterial community under ammonia stress was monitored using the 16S rRNA pyrosequencing and quantitative PCR under similar conditions as in experiment I but without the addition of external propionate. An additional higher ammonium treatment (10 g NH_4^+–N L^{-1}) was applied in experiment II to maximize the ammonia stress. We identified that the *Smithella* bacteria and the *Methanosaetaceae* and *Methanospirillaceae* archaea were the most active players involved in SPO and methanogenesis. We revealed that *Smithella*, *Methanosaetaceae* and *Methanospirillaceae* were moderately and severely inhibited at 3 and 7–10 g NH_4^+–N L^{-1}, respectively. However, the fermentative bacteria appeared to be more tolerant to ammonia stress. The microbial responses were corroborated with the accumulation of VFAs and the repression of methanogenesis under high ammonium conditions.

1. Introduction

Anaerobic digestion (AD) is widely used to degrade organic waste to biogas which helps reduce reliance on fossil fuels, mitigate emission of greenhouse gases, and lower environmental pollution (McKendry, 2002). In methanogenic AD systems, complex organic matter is ultimately converted to methane and carbon dioxide by an orchestration of fermentation, acetogenesis and methanogenesis (Schink, 1997). The acetogenesis step is catalyzed by bacteria that convert substrates such as fatty acids and alcohols into simple compounds such as H_2, CO_2, formate and acetate. This step is endergonic under standard conditions and can process only if the simple compounds produced are consumed by methanogens through a syntrophic association. Therefore, the acetogenesis is regarded to be critical in the AD processes (Junicke et al., 2016; Schink, 1997). Propionate, a key product during anaerobic decomposition, is degraded via the syntrophic propionate oxidation (SPO) which operates at near thermodynamic equilibrium (Stams and Plugge, 2009).

Several syntrophic propionate oxidation bacteria (SPOB) that grow in syntrophy with methanogens have been described, including the Gram-negative (*Syntrophobacter* and *Smithella*) and Gram-positive bacteria (*Pelotomaculum* and *Desulfotomaculum*) isolated from anaerobic digesters (McInerney et al., 2008). These SPOB have been found widespread in anoxic environments, such as peats, wetlands, rice paddy soils, sediments and subsurface petroleum reservoirs (Gan et al., 2012; Gray et al., 2011; Schmidt et al., 2016). Many environmental factors, such as temperature (Gan et al., 2012), hydraulic retention time (HRT) (Zamanzadeh et al., 2013) and levels of propionate (Ariesyady et al., 2007) and trace elements (molybdenum, tungsten and selenium) (Capson-Tojo et al., 2018; Worm et al., 2009) have been found to influence the SPOB communities. Stable isotope probing (SIP) allows the identification of microbial species that incorporate ^{13}C substrates into their DNA or RNA (Radajewski et al., 2000). This powerful technique has been used to investigate the active populations responsible for

* Corresponding author.
E-mail address: luyh@pku.edu.cn (Y. Lu).

https://doi.org/10.1016/j.watres.2018.09.046
0043-1354/

SPO in rice field soils (Gan et al., 2012; Lueders et al., 2004b). However, a direct identification of the microbial populations responsible for SPO in anaerobic digester sludge still remains unavailable.

This limitation of energy conservation predicts that any subtle disturbances to the AD system could affect the functioning of the SPO community and propionate degrading. Accumulation of ammonium produced from the degradation of protein-rich materials is known to inhibits SPO and methanogenesis in the anaerobic digesters that treat livestock manure (Chen et al., 2008; Montag and Schink, 2016), wherein free ammonia is considered to be the main source of ammonium stress (Rajagopal et al., 2013). Under methanogenic conditions, SPO involves at least three different groups of microbes, namely SPOB, hydrogenotrophic methanogens and aceticlastic methanogens. Presumably, inhibition of any individual group would result in an inhibition of the whole SPO process (Capson-Tojo et al., 2017; Stams and Plugge, 2009; Van Velsen, 1979). A consensus seems to have suggested that syntrophic bacteria and methanogenic archaea have different levels of sensitivity to ammonia, but the details appear contradictory. Calli et al. (2005) indicated that SPOB were more sensitive than methanogenic archaea to free ammonia in anaerobic reactors, while other studies suggested just the opposite (Müller et al., 2006; Weaterholm et al., 2011). Wiegant and Zeeman (1986) proposed that it was the inhibition of the hydrogenotrophic methanogens that resulted in an accumulation of propionate, which further inhibited the aceticlastic methanogens. Likewise, the exact responses of either aceticlastic or hydrogenotrophic methanogens to ammonia varied across a few studies (Jarrell et al., 1987; Kato et al., 2014; Westerholm et al., 2012; Zhang et al., 2014).

To gain more insight into the effects of ammonium on microbes involved in SPO and methanogenesis, we conducted two independent laboratory experiments. In the experiment I, RNA-SIP technique was applied to identify the active organisms involved in SPO in a sludge sample collected from a full-scale swine manure digester (Zhang et al., 2014), and in the experiment II a batch experiment with a wide range of ammonium concentrations was conducted to determine the responses of the entire microbial community in fermentation and methanogenesis to ammonia stress.

2. Materials and methods

2.1. Anaerobic incubation

Activated sludge was collected from a full-scale anaerobic bioreactor (continuous stirred-tank reactor) treating swine manure in a livestock farm located in Bei Langzhong Village, Shunyi District, Beijing. The physicochemical characteristics of swine manure and activated sludge are shown in Supplemental Table S1. The sludge, swine manure and the experimental procedures have been described previously (Zhang et al., 2014). Briefly, 10 g sludge and 1 g swine manure (wet weight) were mixed with 30 mL of 50 mM Hepes buffer (N-2-hydroxyethylpiperazine-N′-2-ethanesulfonic acid) in 100-mL glass bottles. This yielded a substrate/inoculum (S/X) ratio of 3.3 in volatile solid (VS) basis. Prior to mixing, the Hepes buffer was supplemented with NH_4Cl to create a final concentration of 0, 3, 7, 10 NH_4^+–N L^{-1}, respectively (referred to as 0-, 3-7- and 10-N treatments) and autoclaved. The pH of the sludge slurries was adjusted to 7.0 with either 1 M HCl or NaOH. The bottles of sludge slurries were then closed with butyl rubber stoppers, flushed with N_2 and incubated under dark at 35 °C.

In experiment I, the sludge slurries were first preincubated at 35 °C for 30 days. Then, the slurries were incubated under the following conditions: a) without propionate, b) with unlabeled propionate and c) with [U–^{13}C] propionate (99 atom%, Sigma-Aldrich, American) at 35 °C for 201 h. Three levels of N were applied, i.e. the 0-, 3- and 7-N treatments. The total amount of propionate for 0-N and 3-N treatments was 8 mM, which was segmented into two doses with equal quantity applied at 0 and 82 h, respectively, for strengthening the ^{13}C labeling. For the 7-N treatment, the addition of 4 mM propionate occurred only once at 0 h. In experiment II, the slurries were incubated for 86 days without preincubation and without addition of propionate. Swine manure added at the beginning was the only substrate for acetogenic and methanogenic activity. An entire range of N concentrations in medium, i.e. 0, 3, 7, 10 g NH_4^+–N L^{-1}, were applied. All incubations were carried out in triplicate.

2.2. Chemical analysis

The gaseous samples were taken form headspace for analyzing the concentration and $^{13}C/^{12}C$ ratios of CH_4 and CO_2 according to the methods previously (Zhang et al., 2014). Liquid samples were collected and centrifuged, then the supernatants were filters and stored at −20 °C as described previously (Zhang et al., 2014). Volatile fatty acids were measured using high performance liquid chromatography (Sykam, Gilching, Germany) with refractive index and UV detectors, with a detection limit of ca. 5 μM ^{13}C abundance in volatile fatty acids from the liquid samples were measured using a HPLC system (Spectra System P1000, Thermo Finnigan, USA) equipped with an ion exclusion column (Aminex HPX-87-H, Bio-Rad, Munich, Germany) and coupled to a Finnigan LC IsoLink (Thermo Electron Corporation, Germany). Isotope ratio values were detected using IRMS (Finigan MAT delta plus advantage) (Penning and Conrad, 2007). The pH of incubation medium and concentration of NH_4^+–N was measured as described previously (Zhang et al., 2014). The free ammonia (NH_3–N) was calculated based on NH_4^+/NH_3 equilibrium, taking into account the concentration of NH_4^+–N, temperature, pH (Rajagopal et al., 2013) and the ionic strength of medium according to Pitzer's ion-interaction approach (Hafner and Bisogni, 2009).

2.3. Nucleic acid extraction and gradient centrifugation

Simultaneous extraction of DNA and RNA in sludge samples was conducted as previously described with modification (Noll et al., 2005). RiboGreen (Invitrogen, American) was used to quantify RNA content in the extracts. The RNA was density resolved by equilibrium density gradient centrifugation in CsTFA (GE Healthcare, American) under the conditions reported previously (Lueders et al., 2004a). After centrifugation, the cesium trifluoroacetate buoyant density of each fraction was determined, and RNA was precipitated and re-suspended in nuclease-free water for subsequent quantitative and qualitative community analyses. Control gradients were conducted with RNA from unlabeled sludge samples. Reverse transcription PCR (RT-PCR) was performed using cDNA Synthesis Kit (TaKaRa), following the protocol described previously (Yuan et al., 2011).

2.4. Quantitative analysis of rRNA

Bacterial and archaeal 16S rRNA from gradient fractions was quantified using quantitative (real-time) PCR in a 7500 real-time PCR system (Applied Biosystems) with the primer pair Ba519f/907r (Lueders et al., 2004a) and Ar364f/934r (Kemnitz et al., 2005) respectively. The standards, that had a dilution series (factor 10) corresponding to 1.2×10^8 to 1.2×10^2 copies μl^{-1}, were prepared from an *in vitro* transcript of bacteria and archaea clones from our sludge samples using the Riboprobe *in vitro* Transcription System

(Promega) according to the manufacture instruction. The RiboGreen RNA quantification kit (Invitrogen, American) was used to quantify the *in vitro* transcript. Each measurement was performed in triplicate. The raw data was analyzed as described previously (Zhang et al., 2014).

2.5. Community analyses

Terminal restriction fragment length polymorphism (T-RFLP) analysis of density-resolved bacterial and archaeal communities from gradient fractions was performed by PCR using primer pairs Ba27f-FAM/Ba907r and Ar109f/Ar934r-FAM, respectively (Lueders et al., 2004a, 2004b). PCRs were performed in 50 μl volumes containing 25 μl of Taq 360 DNA polymerase pre-mix buffer (ABI), 2 μl of each 10 μM primer (Invitrogen) and 1 μl of template. The thermal profile of the PCR for bacterial amplification included 30 cycles of primer annealing at 53 °C for 30 s, primer extension at 72 °C for 1 min and denaturing at 95 °C for 30 s. The final elongation step was 7 min. The thermal profile for archaeal amplification included 32 cycles of primer annealing at 52 °C for 30 s, primer extension at 72 °C for 1 min and denaturing at 94 °C for 30 s. The final elongation step was 7 min. Amplicons were purified and digested by *MspI* (Bacteria) and *TaqI* (Archaea) respectively. The digestion products were then size-separated on an ABI 3730xl DNA analyzer and the data analyzed as described previously (Zhang et al., 2014).

For cloning and sequencing, bacterial and archaeal PCR products from representative cDNA of "heavy" and "light" gradient fractions were purified and ligated into the pGEM-T Easy Vector system (Promega) according to the manufacturer's instructions. After transformation of the plasmids, clones were randomly selected and sequenced with an ABI 3730xl DNA sequencer (Gan et al., 2012). The sequences were assigned to operational taxonomic units (OTUs) based on a sequence similarity cutoff of 97% (bacteria) and 99% (archaea) using the DOTUR and Mothur programs (Schloss et al., 2009). Phylogenetic trees were constructed using neighbor-joining algorithm of the ARB software package (http://www.arb-home.de) for bacteria and Mega 4 program for archaea as described previously (Rui et al., 2009). All sequences have been deposited in GenBank database under accession numbers KJ852774 - KJ853130 (bacteria) and KF670361-KF670564 (archaea).

For pyrosequencing, the V1–V3 region (about 500 bp) of the bacterial 16S rRNA gene was achieved using the primers Ba27f and Ba533r, that containing the eight-base sample specific barcode sequence and the sequencing adaptors (454 Life Sciences). The PCRs were performed in 50 μl volumes containing 10 × PCR Buffer (Promega), 0.2 mM dNTPs (TaKaRa), 10 pmol each primer, 1.5 U of Pfu DNA polymerase (Promega) and 1 μl of template DNA or cDNA. Instrument (Applied Biosystems) with an initial denaturation at 95 °C for 2 min followed by 25 cycles: 95 °C for 30 s (denaturation), 55 °C for 30 s (annealing) and 72 °C for 1 min (extension), and a final extension at 72 °C for 5 min. Negative controls without adding template were also performed during amplifications. Then, PCR products were visualized on agarose gels (2%) and purified with a DNA gel extraction kit (TIANGEN, China). PicoGreen (Invitrogen, American) was used to quantify DNA content in the PCR products, that were also quality controlled on an Agilent 2100 bioanalyzer (Agilent, USA). Then, the amplicons from different samples were pooled in equimolar ratios based on concentration and subjected to emulsion PCR to generate amplicon libraries, as recommended by 454 Life Sciences. Amplicon pyrosequencing was performed using a Roche Genome Sequencer GS FLX Titanium platform at Majorbio Biopharm Technology Co., Ltd., Shanghai, China. The high-throughput amplicon sequencing data of bacterial 16S rRNA was analyzed by QIIME (http://qiime.org) and Mothur (http://www.mothur.org). The unique sequences were clustered into OTUs defined by 97% similarity. All sequences have been deposited in GenBank Short Read Archive (Accession number: PRJNA248031).

3. Results

3.1. Experiment I: bacterial and archaeal RNA-SIP

3.1.1. Oxidation of propionate and methanogenesis

The pH of the sludge slurries became stable after 201 h of incubation (Supplemental Fig. S1A). The pH values for the 0 and 3 g NH_4^+–N L^{-1} (0-N and 3-N) treatments were around 7.1 and 7.0, respectively. In the 7 g NH_4^+–N L^{-1} (7-N) treatment, the pH decreased slightly from 7.0 to 6.9 during the incubation. The lower pH in the 7-N treatment was in accordance with the accumulation of fatty acids. The NH_4^+–N concentrations for all the treatments remained stable through most of the experimental period (Supplemental Fig. S1B). In the later stage, however, NH_3–N concentration decreased because of the decreasing pH (Supplemental Fig. S1C and D).

Propionate produced from the organic compounds in the swine manure sludge was exhausted in the 0- and 3-N treatments after a pre-incubation period of 30 days, but about 4 mM of propionate still remained in the 7-N treatment (Fig. 1C), indicating a substantial inhibition of SPO at the level of 7-N. Nevertheless, all pre-incubated sludge was further incubated with addition of 0.35 mmol ^{12}C- or [U–^{13}C]-propionate (Fig. 1C). In the 0- and 3-N treatments, depletion of propionate occurred at a rate of 3.29 and 1.83 μmol h^{-1}, respectively. By 82 h, 89% and 49% of the added propionate had been depleted in the 0- and 3-N treatments, respectively. At this time, the identical amount of propionate (0.35 mmol) was added again to both treatments to bringing the total addition of ^{12}C- or [U–^{13}C]- propionate to 0.7 mmol. Between 82 and 133 h, the rate of propionate degradation was faster in the 0-N (6.52 μmol h^{-1}) than the 3-N (3.09 μmol h^{-1}) treatments. In contrast, propionate degradation in 7-N treatment was completely inhibited, where the total propionate concentration remained unchanged at about 10 mM in slurries.

The analysis of isotopic carbon ratios revealed that ^{13}C atom% of acetate (Fig. 1E) increased immediately after addition of [U–^{13}C] propionate (Fig. 1F) and peaked at 89% and 68% at 133 h in the 0- and 3-N treatments, respectively. Meanwhile, the total amounts of acetate and formate varied between 0.02 and 0.32 mM and between 0.01 and 0.03 mM, respectively, while the concentration of butyrate was below the detection limit (Fig. 1A, B and D). In contrast, acetate and butyrate accumulated in the 7-N treatment (Fig. 1B, D), while the ^{13}C atom% of acetate and butyrate remained below 2% throughout the incubation (Fig. 1E and G). Apparently, acetate and butyrate in this treatment were resulted from the degradation of complex organic compounds in swine manure sludge rather than the [U–^{13}C] propionate added.

In correspondence with [U–^{13}C] propionate consumption, ^{13}C-labeled CH_4 was produced in the 0- and 3-N treatments. The rate of CH_4 production was faster in the 0-N (6.17 μmol h^{-1}) than 3-N treatment (3.89 μmol h^{-1}) after the first addition of propionate (Fig. 2A). The rates further increased after the second addition of propionate at 82 h, but it was faster again in the 0-N treatment (9.67 μmol h^{-1}) than in the 3-N treatment (4.60 μmol h^{-1}). The accumulative amount of CH_4 eventually reached to about 1 mmol in both treatments. Theoretically, 0.7 mmol propionate could produce 1.23 mmol CH_4, suggesting that up to 80% of the propionate had be stoichiometrically converted to CH_4. In contrast, CH_4 production was completely inhibited in the 7-N treatment. Likewise, much less CO_2 production was produced in the 7-N than the 0-N and 3-N treatments (Fig. 2B). The analysis of isotopic carbon ratios revealed that the ^{13}C content of CH_4 and CO_2 increased with the

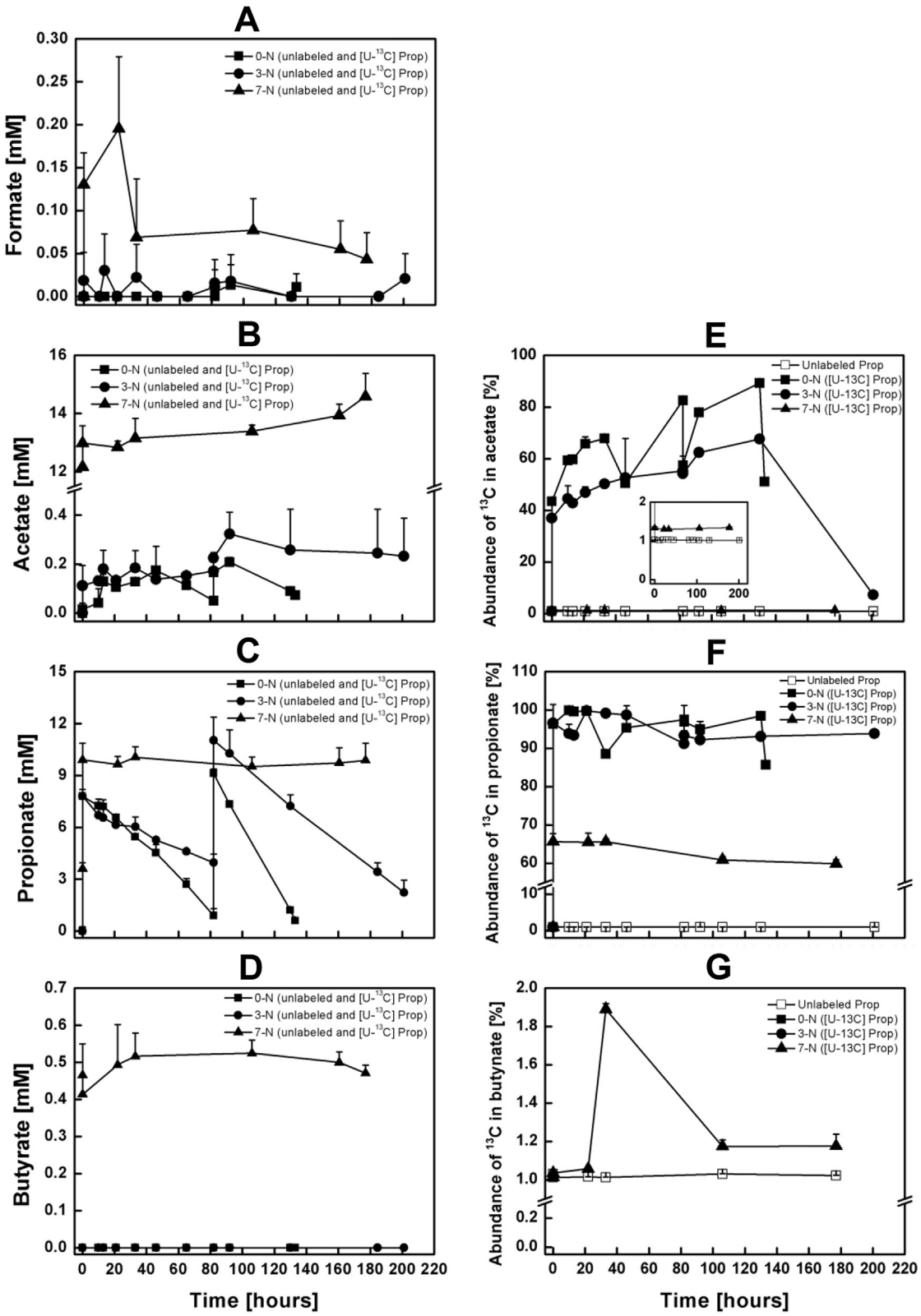

Fig. 1. The time-course of VFA and its ^{13}C abundance in sludge incubations with different ammonium treatments. These include formate (A), acetate (B), propionate (C), butyrate (D), ^{13}C abundance of acetate (E), ^{13}C abundance of propionate (F) and ^{13}C abundance of butyrate (G). Data of VFA concentration, which include ^{12}C (n = 3) and ^{13}C (n = 3) propionate treatments, are mean ± SD (n = 6). Data of VFA ^{13}C abundance are mean ± SD (n = 3).

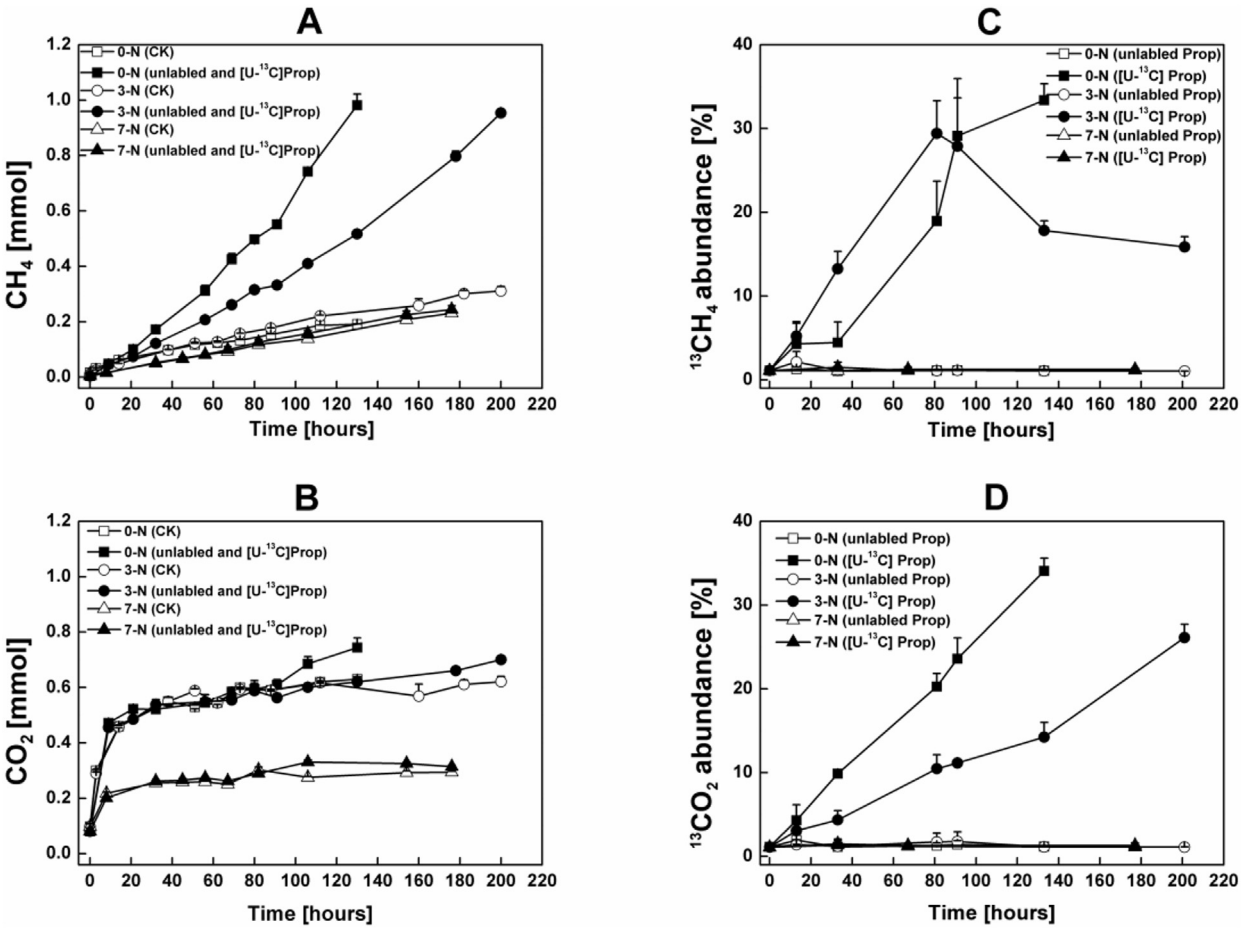

Fig. 2. The time-course of biogas and its ^{13}C abundance with different ammonium treatments. These include CH_4 (A), CO_2 (B), ^{13}C abundance of CH_4 (C) and ^{13}C abundance of CO_2 (D) in sludge incubations CK means the control treatments, which does not add propionate. Data of CH_4 content, which include ^{12}C (n = 3) and ^{13}C (n = 3) propionate treatments, are mean ± SD (n = 6). Data of CK and ^{13}C abundance of CH_4 and CO_2 are mean ± SD (n = 3).

degradation of [U−^{13}C] propionate in the 0- and 3-N treatments and reached the maximum (about 30%) after 133 and 81 h, respectively (Fig. 2C and D). In contrast, the ^{13}C atom% of CH_4 and CO_2 in the 7-N treatment remained below 2% throughout the incubation.

3.1.2. SIP targeting bacterial 16S rRNA

RNA-SIP was applied only for the 0- and 3-N treatments, but with multiple times for each treatment. Fig. 3 shows a time-course analysis of relative abundance of bacterial individual terminal restriction fragments (T-RFs) across the density gradient with either ^{12}C- or ^{13}C-labeled propionate in the 0- and 3-N treatments. In both the labeled and unlabeled treatments for most of the time points, the 195-bp and 520-bp T-RFs were the dominant fragments with a combined relative abundance exceeding 50% across the density gradient (Fig. 3). There was only one obvious T-RF namely the 509-bp that became more abundant at higher density gradients over time in the ^{13}C-labeled treatments (Fig. 3E–G for the 0-N, and Fig. 3d-e for the 3-N). Its relative abundance exceeded 20% at the highest density gradient by the end of the samplings (Fig. 3H for the 0-N and Fig. 3f for the 3-N). In contrast, in the unlabeled control, the relative abundance of the 509-bp T-RF remained below 5% across the RNA buoyant density gradients (Fig. 3A–D for the 0-N, and Fig. 3a-c for the 3-N).

In order to assign the characteristic T-RFs to phylogenetic groups, four clone libraries were constructed from the samples of different buoyant densities at 133 h for the 0-N treatment and 201 h for the 3-N treatment, respectively. Two of the clone libraries were constructed using 'light' templates of rRNA as controls, and two retrieved from the 'heavy' templates.

Phylogenetic analysis of 358 sequences indicated that the bacterial community in the sludge comprised mainly *Firmicutes*, *Proteobacteria*, *Bacteroidetes* and *Chloroflexi* (Supplemental Table S2, and Fig. 4, S2 and S3). *Actinobacteria*, *Spirochaetes*, *Synergistetes* and unclassified lineages had lower abundances. *In silico* T-RF comparisons between 'heavy' and 'light' clone libraries indicated that the 'light' rRNA was dominated by the sequences related to *Clostridia* (520-bp T-RF for *Clostridium* spp., Supplemental Fig. S2), *Peptostreptococcaceae* (195-bp T-RF, Supplemental Fig. S2), *Bacilli* (152- and 533-bp T-RFs, Supplemental Fig. S2) and *Dethiosulfovibrionaceae* (140-bp T-RF, Supplemental Fig. S3), whereas the clone sequences affiliated with *Smithella* (509-bp T-RF, Fig. 4), *Syntrophorhabdaceae* (162-bp T-RF, Fig. 4), *Bacteroidales* (93-bp T-RF, Supplemental Fig. S3) and *Pelotomaculum* (142-bp T-RF, Supplemental Fig. S2) were enriched in the 'heavy' rRNA in the 0- and 3-N treatments.

3.1.3. SIP targeting archaeal 16S rRNA

RNA-SIP was also done to identify the archaeal members that assimilated the intermediate metabolites of [U−^{13}C] propionate during the degradation over time. The T-RFLP analysis of archaeal community showed three major T-RFs of 84, 284 and 393-bp

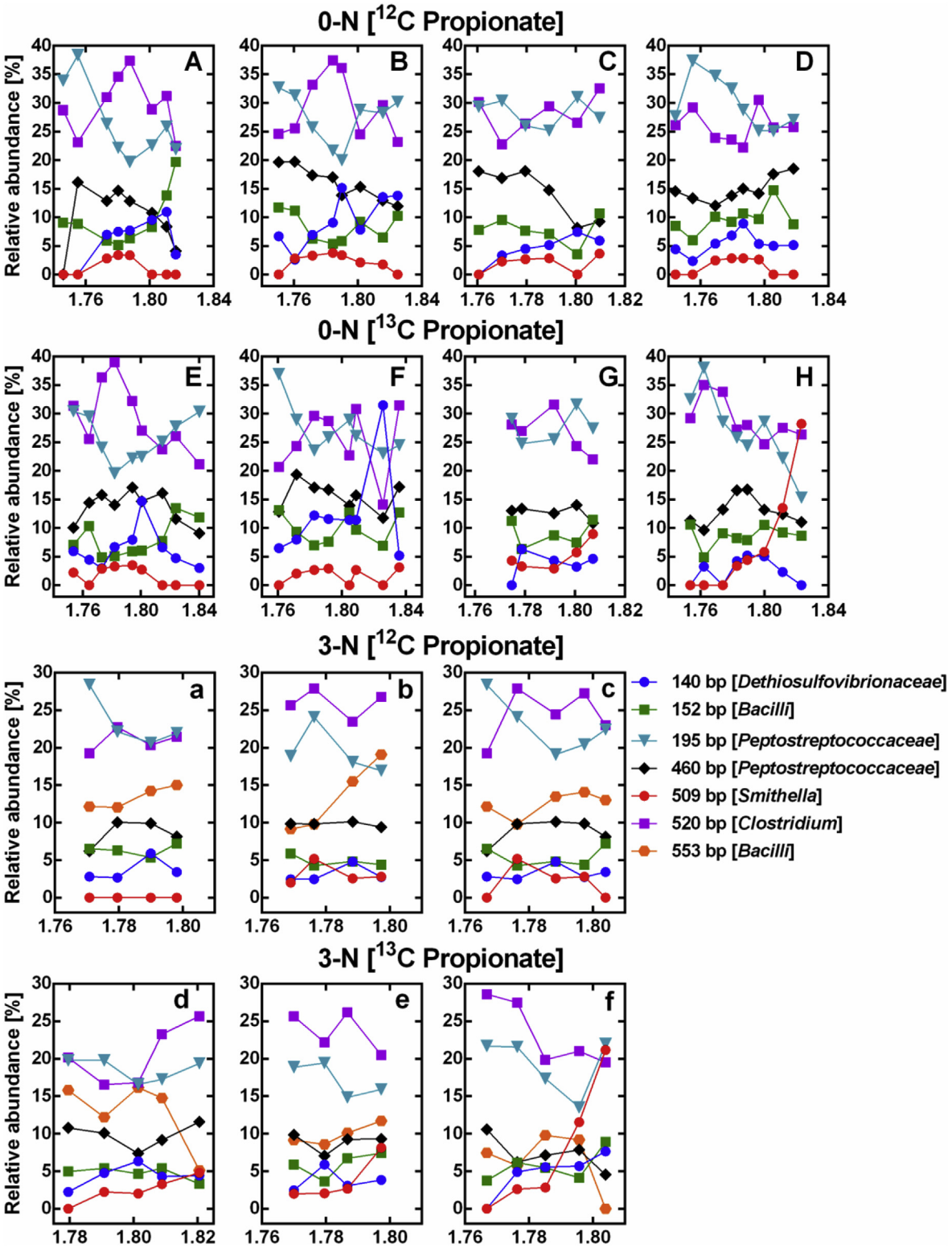

Fig. 3. Relative abundance of different bacterial T-RFs across CsTFA buoyant densities in the 0 and 3 g NH_4^+–N L^{-1} treatments. The sampling time points include 13 h (A, E), 33 h (B, F), 91 h (C, G) and 133 h (D, H) of ^{12}C propionate (A–D) and ^{13}C propionate (E–H) treatments in the 0 g NH_4^+–N L^{-1} sludge incubations. The sampling time points also include 33 h (a, d), 91 h (b, e) and 201 h (c, f) of ^{12}C propionate (a–c) and ^{13}C propionate (d–f) treatments in the 3 g NH_4^+–N L^{-1} sludge incubations.

occurring in both the 0- and 3-N treatments, and a 186-bp T-RF appeared additionally in the 3-N treatment (Fig. 5). In both the ^{12}C- and ^{13}C- treatments and regardless of density gradient, the 284-bp TR-F always predominated with a relative abundance of >60%. Compared with the ^{12}C-controls in the 0-N treatment (Fig. 5A–D), the 393-bp but not the 84-bp T-RF became substantially enriched in the 'heavy' rRNA fractions at 91 h of the ^{13}C-treated slurries (Fig. 5E–G). However, this enrichment of the 393-bp T-RF declined

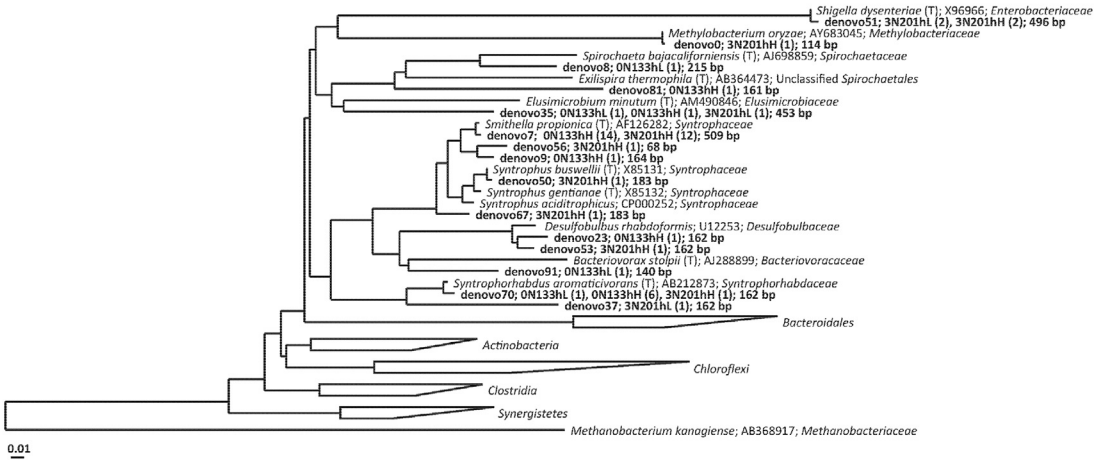

Fig. 4. Phylogenetic relationship of reference bacteria and *Proteobacteria* 16S rRNA gene sequences retrieved from RNA-SIP samples. The 16S rRNA clone libraries were obtained from 'light' buoyant density fraction sample collected on 133 h in the treatment of 0 g NH_4^+–N L^{-1} sludge (referred to as 0N133 hL), 'heavy' fraction sample collected on 133 h in the treatment of 0 g NH_4^+–N L^{-1} sludge (referred to as 0N133 hH), 'light' fraction sample collected on 201 h in the treatment of 3 g NH_4^+–N L^{-1} sludge (referred to as 3N201 hL) and 'heavy' fraction sample collected on 201 h in the treatment of 3 g NH_4^+–N L^{-1} sludge (referred to as 3N201 hH), respectively. The numbers of OTUs (97% identify threshold) are given in the parentheses and the sizes (bp) of terminal restriction fragment (T-RF) are given at the end. The GenBank accession numbers of the reference sequences are also indicated. The scale bar represents 1% sequence divergence.

subsequently at 133 h (Fig. 5H). Instead, the 84-bp T-RF became slightly enriched herein. In the 3-N treatment, a different pattern emerged. It was the 84-bp T-RF that became substantially enriched in the 'heavy' rRNA fractions at both 91 h and 201 h of the ^{13}C-treated slurries (Fig. 5e-f).

Four archaeal 16S rRNA clone libraries were constructed from the 'light' and 'heavy' fractions at 91 h and 201 h in the 0- and 3-N treatments, respectively (Supplemental Table S3). Sequencing analysis of 204 clones indicated that the archaeal community in the sludge consisted of *Methanosaetaceae*, *Methanospirillaceae*, *Methanomicrobiales*, *Methanosarcinaceae* and *Thermoprotei* (Supplemental Fig. S4). Based on *in silico* analysis of these archaeal sequences, the major T-RFs were assigned to *Methanosaetaceae* (284-bp), *Methanospirillaceae* (393-bp), *Methanomicrobiales* (84-bp), and *Methanosarcinaceae* (186-bp), respectively.

3.2. *Experiment* II: NH_4^+ *stress on bacterial communities*

3.2.1. *Dynamics of acetate and propionate*

In experiment II, acetate accumulated and then decomposed rapidly in the 0- and 3-N treatments, with the concentration decreasing to a level near to the detection limit (about 40 μM) in three days (Fig. 6A). In the 7-N treatment, acetate increased to 12 mM on day 6 and remained steady within the next month, then decreased below 0.3 mM at the end of incubation. In the 10-N treatment, acetate kept accumulating and reaching 25 mM at the end of incubation. A similar acetate dynamic has been shown previously (Zhang et al., 2014). Propionate also showed a rapid accumulation in the 0-N treatment but decreased to the level of the detection limit (about 40 μM) in six days (Fig. 6B). In the 3-N treatment, propionate increased to 3.5 mM on day 15 and then decreased rapidly to below 0.4 mM after day 22. In the 7- and 10-N treatments, the propionate kept increasing and reached 6.0 and 4.2 mM, respectively, at day 86.

3.2.2. *Bacterial community dynamics*

Bacterial 16S rRNA genes and their transcripts were extracted from the sludge samples in different ammonia treatments and analyzed by 454 pyrosequencing. Phylogenetic analysis indicated that the bacterial community at the phylum level consisted of *Proteobacteria*, *Firmicutes*, *Bacteroidetes*, *Chloroflexi*, *Actinobacteria*, *Spirochaetes* and *Synergistetes* (Fig. 7). The structure of bacterial community remained relatively stable throughout the incubations (Fig. 7A). The *Firmicutes* predominated in all samples, accounting for >60% of total bacterial abundance. The next major bacterial phyla included *Bacteroidetes*, *Chloroflexi* and *Proteobacteria*. *Bacteroidetes* and *Chloroflexi* accounted for about 10% of total bacterial abundance across treatments. Along with the elevation of the N level, the relative abundance of *Proteobacteria* gradually decreased from about 10% in the 0-N treatment to below 1% in the 10-N treatment.

The relative abundances of bacterial 16S rRNA transcripts revealed some differences from the community composition at the DNA level (Fig. 7B). The *Firmicutes* still predominated in all samples, accounting for over 70% of the total bacterial transcripts in the 0-N treatment. However, it increased along with the elevation of the N level and peaked at 92% in the 10-N treatment. The relative abundance of the *Bacteroidetes* and *Chloroflexi* was lower at the RNA level than at the DNA level and decreased in response to the increasing N concentration. The relative abundance of the *Proteobacteria* was moderately higher at the RNA level in the 0-N and 3-N treatments, making it the second group of transcriptionally most active organisms after the *Firmicutes*. However, it decreased below 1% in the 7- and 10-N treatments. Notably, *Smithella* was the dominant genus in the *Proteobacteria*.

At the lower taxonomic levels (family or genus), the 16S rRNA sequences closely related to *Smithella* and *Syntrophorhabdaceae* were dominant in the clone libraries. The relative abundances of their 16S rRNA genes and transcripts were calculated and compared among different N levels (Fig. 8 and Supplemental Fig. S5). In general, the relative abundances of *Smithella* and *Syntrophorhabdaceae* were highest in the 0-N treatment, reaching to 3.9% and 5.0% for the 16S rRNA genes and transcripts of *Smithella* and 1.8% and 2.2% for those of *Syntrophorhabdaceae*, respectively. Furthermore, the relative abundances of two groups at both gene and transcript levels increased with the time of incubation in this treatment. The relative abundances at the gene level, however, decreased with the increase of ammonium concentration (Fig. 8A

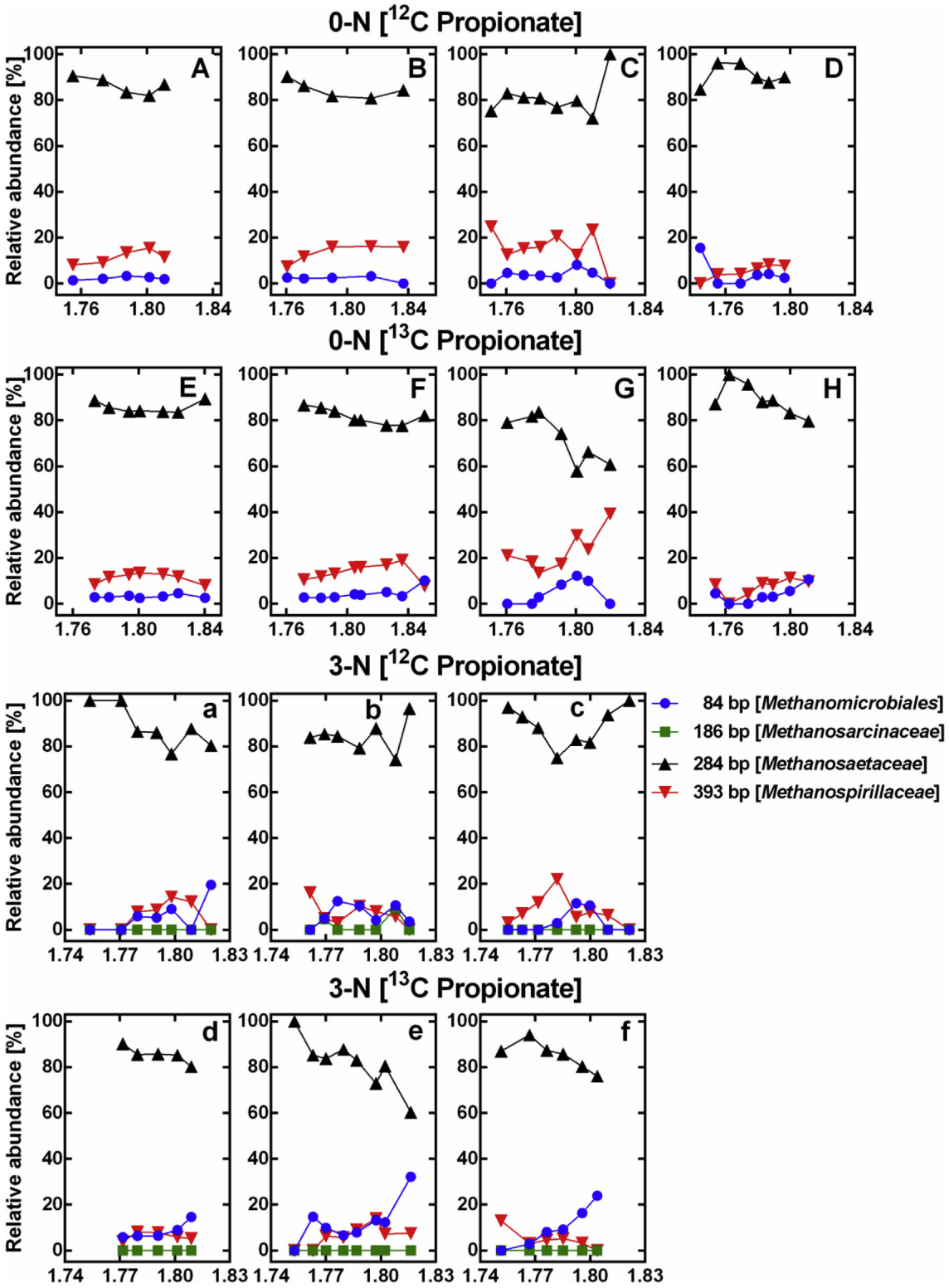

Fig. 5. Relative abundance of different archaeal T-RFs across CsTFA buoyant densities in the 0 and 3 g NH_4^+–N L^{-1} treatments. The sampling time points include 13 h (A, E), 33 h (B, F), 91 h (C, G) and 133 h (D, H) of ^{12}C propionate (A–D) and ^{13}C propionate (E–H) treatments in the 0 g NH_4^+–N L^{-1} sludge incubations. The sampling time points also include 33 h (a, d), 91 h (b, e) and 201 h (c, f) of ^{12}C propionate (a–c) and ^{13}C propionate (d–f) treatments in the 3 g NH_4^+–N L^{-1} sludge incubations.

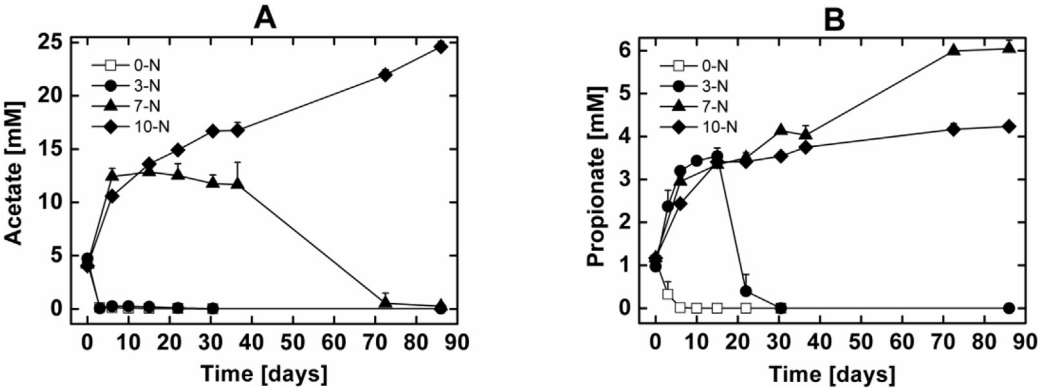

Fig. 6. The time-course of acetate (A) and propionate (B) in sludge incubations with the 0, 3, 7 and 10 g NH_4^+–N L^{-1} treatments. Data are mean ± SD (n = 3).

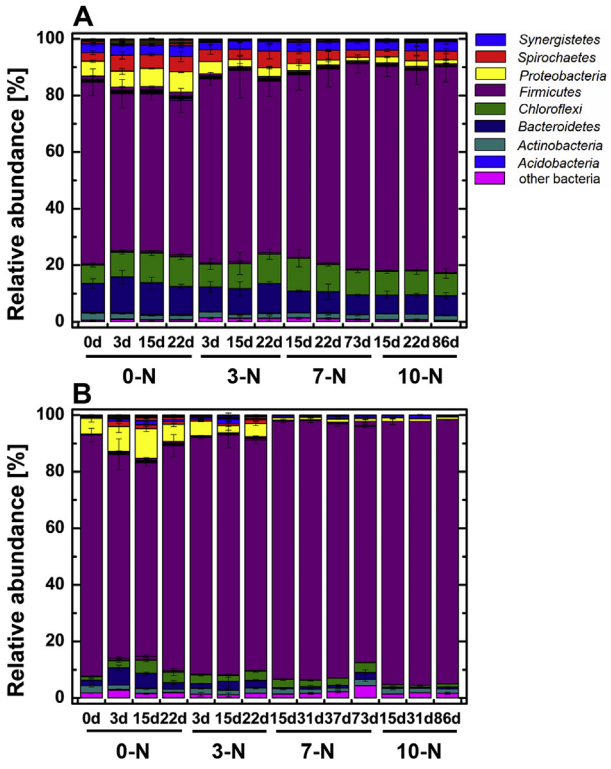

Fig. 7. Relative abundance of bacterial composition at phylum level. Data was from 454 pyrosequencing analyses targeting of bacterial 16S rRNA genes (A) and transcripts (B). Data are mean ± SD (n = 3).

and C) and did not show a clear tendency over the incubation time for the 3-, 7- and 10-N treatments. The decline tendency with the increase of NH_4^+–N was more substantial at the transcript level. Notably, while *Smithella* and *Syntrophorhabdaceae* kept a moderate abundances of their 16S rRNA genes, their transcript abundances were close to zero at the 7-N and 10-N levels.

3.2.3. Dynamics of total bacterial 16S rRNA gene copy numbers

The total bacterial 16S rRNA gene copy numbers estimated by quantitative PCR ranged from 3.2×10^{11} to 1.9×10^{12} copies g^{-1} sludge (dw) (Fig. 9A). Within the low-N treatments, the copy number increased over time at the early stage, then decreased after day 10. The total 16S rRNA gene copy numbers exhibited the significant difference between the low-N and high-N treatments (Fig. 9B). But there was no significant difference either between the 0- and 3-N treatments or between the 7- and 10-N treatments (Fig. 9B).

4. Discussions

4.1. Impacts of ammonia on propionate oxidation and methanogenesis

In the present study, we showed that the average rates of propionate consumption and methane production decreased from 4.9 to 7.52 μmol h^{-1} in the 0-N treatment to 2.36 and 4.75 μmol h^{-1} in the 3-N treatment, or reduced by 52% and 37%, respectively. In the 7-N treatment (7 g NH_4^+–N L^{-1}, corresponding to 69 mg NH_3–N L^{-1}), both propionate degradation and methane production were completely inhibited. These results are in line with a previous study that reported 48% reduction in CH_4 production rate when the total ammonia/ammonium nitrogen (TAN) concentration increased from 3 to 5.8 g l^{-1} in a continuously stirrer tank reactor (Sung and Liu, 2003). On the other hand, the existence of propionate degraders resistant to the extremely high ammonium concentration (6 g NH_4^+–N L^{-1}) in anaerobic bioreactors has been reported (Calli et al., 2005). However, such resistance was not observed in our study (Fig. 8).

Propionate and acetate transiently accumulated and were depleted thereafter in the 0- and 3-N treatments (Fig. 1B and C). In the 10-N treatment, however, propionate and acetate accumulated throughout the incubation (Fig. 6A–B), suggesting a strong inhibition on the degradation of propionate and acetate. The 7-N treatment exhibited an interesting pattern in experiment II, where acetate (Fig. 6A) decreased gradually in the later stage of incubation while propionate kept accumulating. This suggests that consumption of acetate alone would not be sufficient for the resumption of propionate degradation. In a previous study, we showed that hydrogen accumulated to a significant extent in high NH_4^+ treatments (Zhang et al., 2014)). The H_2 accumulation may build a stronger thermodynamic barrier for the degradation of propionate.

4.2. SPOB and their responses to ammonia stress

In soil and sediment samples, biomass usually can be sufficiently labeled after the incorporation of 5–500 μmol ^{13}C per g (Whiteley et al., 2007). Since microbial biomass in anaerobic sludge is often richer, a ^{13}C amount in the higher range would probably be needed. In our experiment I, the concentration of ^{13}C-labeled propionate was about 8 mM (about 400 μmol ^{13}C per g dw sludge). This not

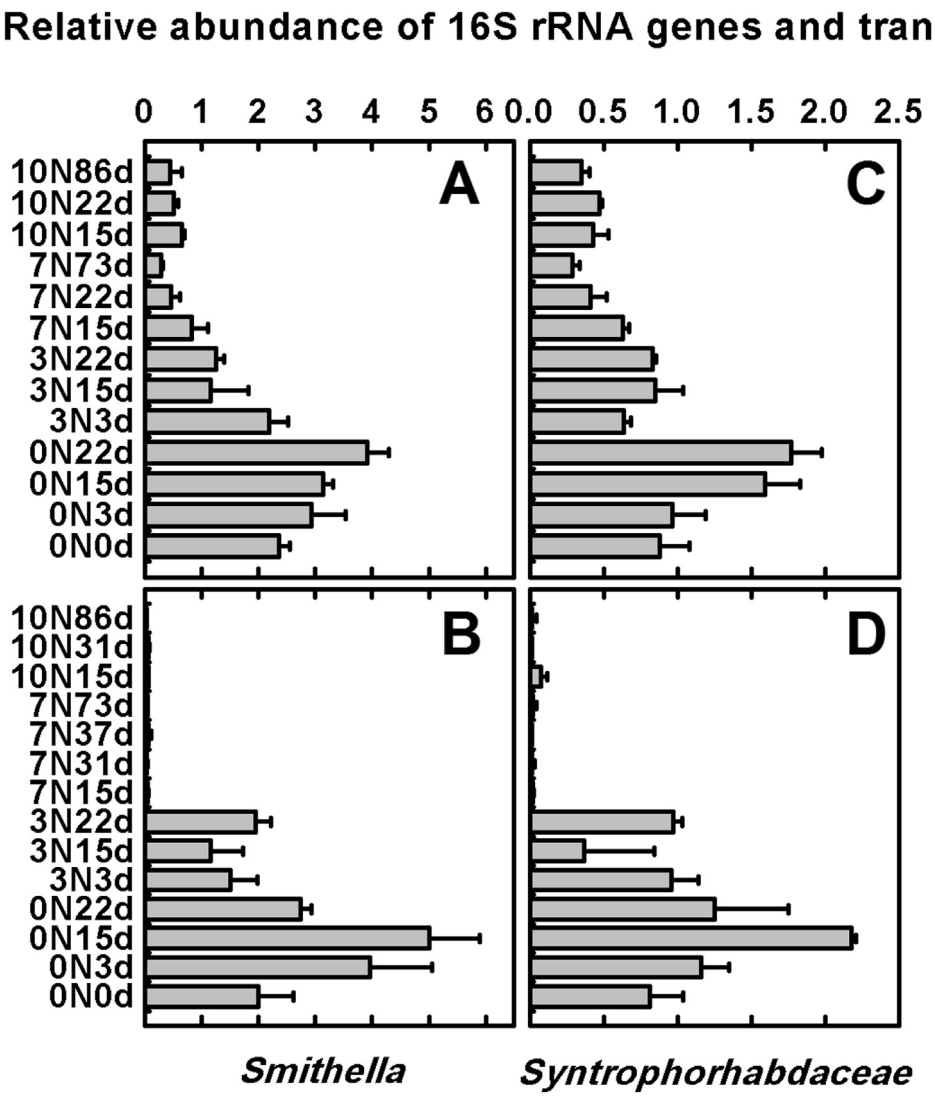

Fig. 8. The relative abundances of 16S rRNA genes (A and C) and transcripts (B and D) for the *Smithella* (A and B) and *Syntrophorhabdaceae* (C and D), respectively. Data were retrieved from 454 pyrosequencing of the constructed clone libraries. Note the different scales for *Smithella* and *Syntrophorhebedaceae*. Data are mean ± SD (n = 3).

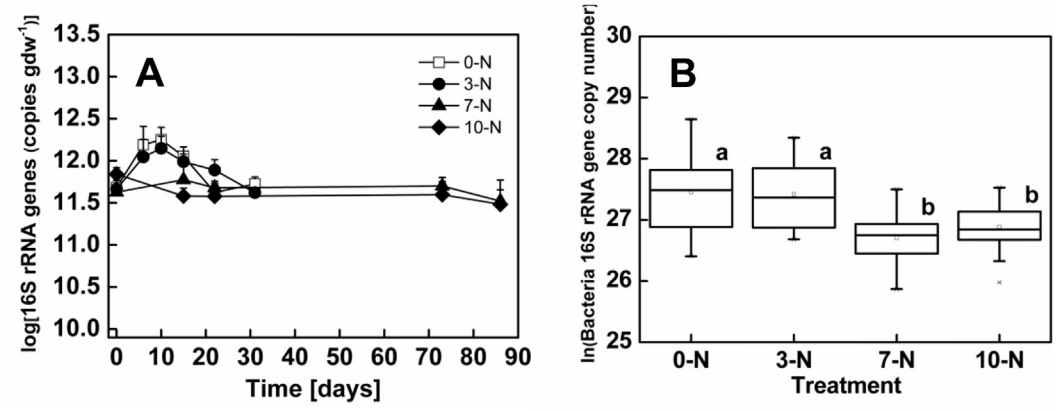

Fig. 9. Quantitative PCR (A) and Box-chart (B) analyses based on bacteria 16S rRNA gene copy numbers. Data are mean ± SD (n = 3). Different letters above the boxes indicate a significant difference ($P < 0.01$).

only ensured sufficient labeling, but also was within the 6–8 mM range commonly reached in anaerobic digesters (Van Velsen, 1979).

RNA-SIP revealed that *Smithella*, *Pelotomaculum*, *Syntrophorhabdaceae* and *Bacteroidales* incorporated the propionate-derived ^{13}C into their rRNA in the 0- and 3-N treatments. Among these, *Smithella* were ^{13}C labeled more quickly and to a significantly higher extent, indicating the significance of *Smithella* as the key SPOB in the swine manure sludge. Two probable reasons may explain why the *Smithella* had a selective advantage over other SPOB such as *Pelotomaculum* and *Syntrophobacter* (de Bok et al., 2005; Imachi et al., 2007).

First, members of *Smithella* may adapt well to a wide range of environmental conditions. This is supported by their distribution in very different habitats including rice field soils (Gan et al., 2012; Lueders et al., 2004b), wetland (Chauhan and Ogram, 2006), anaerobic digester sludge (Ariesyady et al., 2007) and hydrocarbon-contaminated aquifer or oil sands (Embree et al., 2014; Gray et al., 2011). They may also play important roles in the metabolism of compounds other than propionate (Ariesyady et al., 2007), including butyrate (Liu et al., 1999), crotonic acid (Liu et al., 1999), naphtha (Siddique et al., 2012), *n*-alkane (Gray et al., 2011; Wawrik et al., 2016), BTEX (benzene, toluene, ethylbenzene, and xylenes) (Siddique et al., 2012) and oil (Gray et al., 2011). In addition, in a long-term absence of trace metals (Mo, W and Se), *Smithella propionica* outcompeted *Syntrophobacter* spp. for propionate consumption in a UASB reactor (Worm et al., 2009).

Second, it has been shown that *Smithella* spp. oxidize propionate to acetate and butyrate via the six-carbon dismutation pathway (de Bok et al., 2001). This pathway has the thermodynamic and energetic advantages over the classical methylmalonyl coenzyme A, or the MMA pathway, operating in *Syntrophobacter* and *Pelotomaculum*. The Gibbs free energy change of the MMA pathway (Eq. (1)) is more positive (+71.7 kJ/mol propionate) (Stams and Plugge, 2009) than the dismutation pathway (Eq. (2)) ($\Delta G^{\circ\prime} = +0.12$ kJ/mol) (Liu et al., 1999), and the further oxidation of the butyrate intermediate (Eq. (3)) is less endergonic ($\Delta G^{\circ\prime} = +48.3$ kJ/mol) compared with the MMA pathway. Consequently, a low thermodynamic sensitivity toward H_2 of the dismutation pathway has been indicated that is believed to improve the precarious stability of propionate degradation in methanogenic waste treatment systems (Dolfing, 2013).

$$CH_3CH_2COO^- + 2H_2O \rightarrow CH_3COO^- + CO_2 + 3H_2 \quad (1)$$

$$2CH_3CH_2COO^- \rightarrow CH_3COO^- + CH_3CH_2CH_2COO^- \quad (2)$$

$$CH_3CH_2CH_2COO^- + 2H_2O \rightarrow 2CH_3COO^- + H^+ + 2H_2 \quad (3)$$

Several other T-RFs that also increased in the 'heavy' rRNA fractions belonged to *Syntrophorhabdaceae* in the 0-N treatment and *Bacteroidales* in the 3-N treatment, respectively (Supplemental Table S2). As a representative of the *Syntrophorhabdaceae*, *Syntrophorhabdus aromaticivorans* strain UI was isolated from a mesophilic digester treating aromatic compound-containing wastewater, and the strain was known to syntrophically oxidize aromatic compounds (*p*-cresol, 4-hydroxybenzoate, isophthalate, and benzoate) with a hydrogenotrophic methanogen (Qiu et al., 2008). Phylogenetic analysis indicated that *Syntrophorhabdaceae* was closely related to the *Syntrophaceae* family comprised of *Smithella* and *Syntrophus* (Fig. 4). *Bacteroidales* are widespread in AD systems and are possibly involved in various fermentations (Na et al., 2009). In a DNA-SIP experiment labeled with ^{13}C-Glucose, sequences related to the family *Porphyromonadaceae* (of *Bacteroidetes*) were retrieved in a large number from the 'heavy' DNA library, suggesting the involvement of *Bacteroidetes* in saccharide fermentation (Li et al., 2009). Whether the ^{13}C-labeling of *Syntrophorhabdaceae* and *Bacteroidales* in the present study was due to cross feeding or their direct functioning in SPO deserves further examinations.

4.3. Response of methanogens to ammonia stress

Theoretically, the SPO and methanogenesis processes would be inhibited if any functional group of the microbial consortia involved, namely SPOB, hydrogenotrophic methanogens, aceticlastic methanogens, was inhibited by ammonia (Stams and Plugge, 2009). In our study, not only the activity of the main SPOB (*Smithella*) (Fig. 8A and B) but also those of aceticlastic and hydrogenotrophic methanogens were suppressed at high NH_4^+ concentrations.

The predominance of *Methanosaetaceae* in our incubations (Fig. 5) is consistent with previous studies showing that these aceticlastic methanogens are prevalent in anaerobic wastes digesters and play an important role in methanogenesis and SPO (Ariesyady et al., 2007). *Methanosaetaceae* spp. can consume acetate down to a concentration of 5–20 μM, creating a thermodynamic favorable condition for the SPO (Dong et al., 1994). It has been reported that SPO was suppressed by 50% if acetate accumulated to a concentration of 20 mM (Felchner-Zwirello et al., 2013). The filamentous morphology of *Methanosaeta* spp. can facilitate the formation of microbial aggregates (granular sludge), which has been considered to be critical for the success of anaerobic treatment of waste waters (De Vrieze et al., 2013; Lettinga, 1995; Lyu and Liu, 2018; Sieber et al., 2014). Furthermore, *Methanosaetaceae* might be more metabolically and functionally diverse than previously thought (Smith and Ingram-Smith, 2007). Apart from acetate, the consumption of hydrogen or formate is critical to allow the degradation of propionate to be thermodynamically feasible (Stams and Plugge, 2009). We found that the hydrogenotrophic *Methanospirillum* spp. possibly play the key role in the methanogenesis from SPO. The suppression of ammonia on *Methanosaetaceae* and *Methanospirillaceae* can be the main reason for the dysfunction of methanogenesis and SPO in the swine manure digester sludge.

4.4. Effects on other fermenting bacteria

Studies conducted with both pure cultures and in situ anaerobic digesters have shown that the bacterial communities have a higher tolerance to ammonia toxicity than methanogenic archaea (Müller et al., 2006, 2016; Westerholm et al., 2012). It has been demonstrated that ammonium is not detrimental to at least three model bacterial species (*Corynebacterium glutamicum*, *Escherichia coli*, and *Bacillus subtilis*) even at the level of molar concentrations ($1M = 28$ g NH_4^+–N L^{-1}) (Müller et al., 2006). In a previous study on methanogenic anaerobic digesters, the copy numbers of archaeal 16S rRNA genes started to decrease at 3 g of NH_4^+–N L^{-1}, but the bacterial 16S rRNA copy numbers still remained steady even if the ammonium reached up to 9 g NH_4^+–N L^{-1} (Sawayama et al., 2004).

In our study, the similar results were observed. The fermentative *Firmicutes* such as *Clostridium* spp. and *Peptostreptococcaceae* showed an increase of their 16S rDNA and rRNA relative abundances in the high N treatments and their activities were evidenced with the continuous production of short-chain fatty acids (Figs. 7 and 9). These results suggest that these fermentative bacteria are relatively tolerant to ammonia toxicity in contrast to SPOB and methanogens, i.e. *Smithella*, *Methanosaetaceae* and *Methanospirillaceae*.

5. Conclusions

The conclusions drawn from the present work are summarized as follows:

- The rate of propionate degradation and CH_4 production substantially reduced with the increase of ammonium addition and was completely inhibited if the concentration increased to >7 g NH_4^+–N L^{-1}.
- The *Smithella* bacteria and *Methanosaetaceae* and *Methanospirillaceae* archaea were the key players that participated in SPO and methanogenesis in the swine manure sludges.
- The suppression of ammonia on *Methanosaetaceae* and *Methanospirillaceae* might significantly affect methanogenesis that in turn inhibited the SPO, resulting in the accumulation of propionate.
- Taken together, out results would help to understand the inhibitory effects of ammonia on syntrophic propionate oxidation in anaerobic digester sludges.

Acknowledgment

We thank Marc G. Dumont for the assistance and advice in SIP experiment. We are also in debt to Zhe Lyu for his insightful discussion and review during the manuscript preparation. This study was financially supported by the National Natural Science Foundation of China (grant no. 41630857; 41501251) and the National Key Research and Development Program of China (grant no. 2016YFD0200306).

Appendix A. Supplementary data

Supplementary data to this article can be found online at https://doi.org/10.1016/j.watres.2018.09.046.

References

Ariesyady, H.D., Ito, T., Yoshiguchi, K., Okabe, S., 2007. Phylogenetic and functional diversity of propionate-oxidizing bacteria in an anaerobic digester sludge. Appl. Microbiol. Biotechnol. 75 (3), 673–683.
Calli, B., Mertoglu, B., Inanc, B., Yenigun, O., 2005. Effects of high free ammonia concentrations on the performances of anaerobic bioreactors. Process Biochem. 40 (3–4), 1285–1292.
Capson-Tojo, G., Moscoviz, R., Ruiz, D., Santa-Catalina, G., Trably, E., Rouez, M., Crest, M., Steyer, J.P., Bernet, N., Delgenes, J.P., Escudie, R., 2018. Addition of granular activated carbon and trace elements to favor volatile fatty acid consumption during anaerobic digestion of food waste. Bioresour. Technol. 260, 157–168.
Capson-Tojo, G., Ruiz, D., Rouez, M., Crest, M., Steyer, J.P., Bernet, N., Delgenes, J.P., Escudie, R., 2017. Accumulation of propionic acid during consecutive batch anaerobic digestion of commercial food waste. Bioresour. Technol. 245 (Pt A), 724–733.
Chauhan, A., Ogram, A., 2006. Fatty acid-oxidizing consortia along a nutrient gradient in the Florida Everglades. Appl. Environ. Microbiol. 72 (4), 2400–2406.
Chen, Y., Cheng, J.J., Creamer, K.S., 2008. Inhibition of anaerobic digestion process: a review. Bioresour. Technol. 99 (10), 4044–4064.
de Bok, F.A., Harmsen, H.J., Plugge, C.M., de Vries, M.C., Akkermans, A.D., de Vos, W.M., Stams, A.J., 2005. The first true obligately syntrophic propionate-oxidizing bacterium, *Pelotomaculum schinkii* sp. nov., co-cultured with *Methanospirillum hungatei*, and emended description of the genus *Pelotomaculum*. Int. J. Syst. Evol. Microbiol. 55 (Pt 4), 1697–1703.
de Bok, F.A., Stams, A.J., Dijkema, C., Boone, D.R., 2001. Pathway of propionate oxidation by a syntrophic culture of *Smithella propionica* and *Methanospirillum hungatei*. Appl. Environ. Microbiol. 67 (4), 1800–1804.
De Vrieze, J., De Lathouwer, L., Verstraete, W., Boon, N., 2013. High-rate iron-rich activated sludge as stabilizing agent for the anaerobic digestion of kitchen waste. Water Res. 47 (11), 3732–3741.
Dolfing, J., 2013. Syntrophic propionate oxidation via butyrate: a novel window of opportunity under methanogenic conditions. Appl. Environ. Microbiol. 79 (14), 4515–4516.
Dong, X., Plugge, C.M., Stams, A.J., 1994. Anaerobic degradation of propionate by a mesophilic acetogenic bacterium in coculture and triculture with different methanogens. Appl. Environ. Microbiol. 60 (8), 2834–2838.
Embree, M., Nagarajan, H., Movahedi, N., Chitsaz, H., Zengler, K., 2014. Single-cell genome and metatranscriptome sequencing reveal metabolic interactions of an alkane-degrading methanogenic community. ISME J. 8 (4), 757–767.
Felchner-Zwirello, M., Winter, J., Gallert, C., 2013. Interspecies distances between propionic acid degraders and methanogens in syntrophic consortia for optimal hydrogen transfer. Appl. Microbiol. Biotechnol. 97 (20), 9193–9205.
Gan, Y., Qiu, Q., Liu, P., Rui, J., Lu, Y., 2012. Syntrophic oxidation of propionate in rice field soil at 15 and 30°C under methanogenic conditions. Appl. Environ. Microbiol. 78 (14), 4923–4932.
Gray, N.D., Sherry, A., Grant, R.J., Rowan, A.K., Hubert, C.R., Callbeck, C.M., Aitken, C.M., Jones, D.M., Adams, J.J., Larter, S.R., Head, I.M., 2011. The quantitative significance of *Syntrophaceae* and syntrophic partnerships in methanogenic degradation of crude oil alkanes. Environ. Microbiol. 13 (11), 2957–2975.
Hafner, S.D., Bisogni, J.J., 2009. Modeling of ammonia speciation in anaerobic digesters. Water Res. 43 (17), 4105–4114.
Imachi, H., Sakai, S., Ohashi, A., Harada, H., Hanada, S., Kamagata, Y., Sekiguchi, Y., 2007. *Pelotomaculum propionicicum* sp. nov., an anaerobic, mesophilic, obligately syntrophic, propionate-oxidizing bacterium. Int. J. Syst. Evol. Microbiol. 57 (Pt 7), 1487–1492.
Jarrell, K.F., Saulnier, M., Ley, A., 1987. Inhibition of methanogenesis in pure cultures by ammonia, fatty acids, and heavy metals, and protection against heavy metal toxicity by sewage sludge. Can. J. Microbiol. 33 (6), 551–554.
Junicke, H., Feldman, H., Van Loosdrecht, M.C., Kleerebezem, R., 2016. Limitation of syntrophic coculture growth by the acetogen. Biotechnol. Bioeng. 113 (3), 560–567.
Kato, S., Sasaki, K., Watanabe, K., Yumoto, I., Kamagata, Y., 2014. Physiological and transcriptomic analyses of the thermophilic, aceticlastic methanogen *Methanosaeta thermophila* responding to ammonia stress. Microb. Environ. 29 (2), 162–167.
Kemnitz, D., Kolb, S., Conrad, R., 2005. Phenotypic characterization of Rice Cluster III archaea without prior isolation by applying quantitative polymerase chain reaction to an enrichment culture. Environ. Microbiol. 7 (4), 553–565.
Lettinga, G., 1995. Anaerobic digestion and wastewater treatment systems. Antonie Leeuwenhoek 67 (1), 3–28.
Li, T., Mazeas, L., Sghir, A., Leblon, G., Bouchez, T., 2009. Insights into networks of functional microbes catalysing methanization of cellulose under mesophilic conditions. Environ. Microbiol. 11 (4), 889–904.
Liu, Y., Balkwill, D.L., Aldrich, H.C., Drake, G.R., Boone, D.R., 1999. Characterization of the anaerobic propionate-degrading syntrophs *Smithella propionica* gen. nov., sp. nov. and *Syntrophobacter wolinii*. Int. J. Syst. Bacteriol. 49 Pt 2, 545–556.
Lueders, T., Manefield, M., Friedrich, M.W., 2004a. Enhanced sensitivity of DNA- and rRNA-based stable isotope probing by fractionation and quantitative analysis of isopycnic centrifugation gradients. Environ. Microbiol. 6 (1), 73–78.
Lueders, T., Pommerenke, B., Friedrich, M.W., 2004b. Stable-isotope probing of microorganisms thriving at thermodynamic limits: syntrophic propionate oxidation in flooded soil. Appl. Environ. Microbiol. 70 (10), 5778–5786.
Lyu, Z., Liu, Y., 2018. Diversity and Taxonomy of Methanogens, Biogenesis of Hydrocarbons. Handbook of Hydrocarbon and Lipid Microbiology, pp. 1–59.
McInerney, M.J., Struchtemeyer, C.G., Sieber, J., Mouttaki, H., Stams, A.J., Schink, B., Rohlin, L., Gunsalus, R.P., 2008. Physiology, ecology, phylogeny, and genomics of microorganisms capable of syntrophic metabolism. Ann. N. Y. Acad. Sci. 1125, 58–72.
McKendry, P., 2002. Energy production from biomass (Part 1): overview of biomass. Bioresour. Technol. 83 (1), 37–46.
Montag, D., Schink, B., 2016. Biogas process parameters–energetics and kinetics of secondary fermentations in methanogenic biomass degradation. Appl. Microbiol. Biotechnol. 100 (2), 1019–1026.
Müller, B., Sun, L., Westerholm, M., Schnürer, A., 2016. Bacterial community composition and fhs profiles of low- and high-ammonia biogas digesters reveal novel syntrophic acetate-oxidising bacteria. Biotechnol. Biofuels 9, 48.
Müller, T., Walter, B., Wirtz, A., Burkovski, A., 2006. Ammonium toxicity in bacteria. Curr. Microbiol. 52 (5), 400–406.
Na, H., Kim, S., Moon, E.Y., Chun, J., 2009. *Marinifilum fragile* gen. nov., sp. nov., isolated from tidal flat sediment. Int. J. Syst. Evol. Microbiol. 59 (Pt 9), 2241–2246.
Noll, M., Matthies, D., Frenzel, P., Derakshani, M., Liesack, W., 2005. Succession of bacterial community structure and diversity in a paddy soil oxygen gradient. Environ. Microbiol. 7 (3), 382–395.
Penning, H., Conrad, R., 2007. Quantification of carbon flow from stable isotope fractionation in rice field soils with different organic matter content. Org. Geochem. 38, 2058–2068.
Qiu, Y.L., Hanada, S., Ohashi, A., Harada, H., Kamagata, Y., Sekiguchi, Y., 2008. *Syntrophorhabdus aromaticivorans* gen. nov., sp. nov., the first cultured anaerobe capable of degrading phenol to acetate in obligate syntrophic associations with a hydrogenotrophic methanogen. Appl. Environ. Microbiol. 74 (7), 2051–2058.
Radajewski, S., Ineson, P., Parekh, N.R., Murrell, J.C., 2000. Stable-isotope probing as a tool in microbial ecology. Nature 403 (6770), 646–649.
Rajagopal, R., Masse, D.I., Singh, G., 2013. A critical review on inhibition of anaerobic digestion process by excess ammonia. Bioresour. Technol. 143, 632–641.
Rui, J., Peng, J., Lu, Y., 2009. Succession of bacterial populations during plant residue decomposition in rice field soil. Appl. Environ. Microbiol. 75 (14), 4879–4886.
Sawayama, S., Tada, C., Tsukahara, K., Yagishita, T., 2004. Effect of ammonium addition on methanogenic community in a fluidized bed anaerobic digestion. J. Biosci. Bioeng. 97 (1), 65–70.

Schink, B., 1997. Energetics of syntrophic cooperation in methanogenic degradation. Microbiol. Mol. Biol. Rev. 61 (2), 262–280.
Schloss, P.D., Westcott, S.L., Ryabin, T., Hall, J.R., Hartmann, M., Hollister, E.B., Lesniewski, R.A., Oakley, B.B., Parks, D.H., Robinson, C.J., Sahl, J.W., Stres, B., Thallinger, G.G., Van Horn, D.J., Weber, C.F., 2009. Introducing mothur: open-source, platform-independent, community-supported software for describing and comparing microbial communities. Appl. Environ. Microbiol. 75 (23), 7537–7541.
Schmidt, O., Hink, L., Horn, M.A., Drake, H.L., 2016. Peat: home to novel syntrophic species that feed acetate- and hydrogen-scavenging methanogens. ISME J. 10 (8), 1954–1966.
Siddique, T., Penner, T., Klassen, J., Nesbo, C., Foght, J.M., 2012. Microbial communities involved in methane production from hydrocarbons in oil sands tailings. Environ. Sci. Technol. 46 (17), 9802–9810.
Sieber, J.R., Le, H.M., McInerney, M.J., 2014. The importance of hydrogen and formate transfer for syntrophic fatty, aromatic and alicyclic metabolism. Environ. Microbiol. 16 (1), 177–188.
Smith, K.S., Ingram-Smith, C., 2007. *Methanosaeta*, the forgotten methanogen? Trends Microbiol. 15 (4), 150–155.
Stams, A.J., Plugge, C.M., 2009. Electron transfer in syntrophic communities of anaerobic bacteria and archaea. Nat. Rev. Microbiol. 7 (8), 568–577.
Sung, S., Liu, T., 2003. Ammonia inhibition on thermophilic anaerobic digestion. Chemosphere 53 (1), 43–52.
Van Velsen, A.F.M., 1979. Adaptation of methanogenic sludge to high ammonia-nitrogen concentrations. Water Res. 13 (10), 995–999.
Wawrik, B., Marks, C.R., Davidova, I.A., McInerney, M.J., Pruitt, S., Duncan, K.E., Suflita, J.M., Callaghan, A.V., 2016. Methanogenic paraffin degradation proceeds via alkane addition to fumarate by '*Smithella*' spp. mediated by a syntrophic coupling with hydrogenotrophic methanogens. Environ. Microbiol. 18 (8), 2604–2619.
Weaterholm, M., Dolfing, J., Sherry, A., Gray, N.D., Head, L.M., Schnürer, A., 2011. Quantification of syntrophic acetate-oxidizing microbial communities in biogas processes. Environ. Microbiol. Rep. 3 (4), 500–505.
Westerholm, M., Leven, L., Schnürer, A., 2012. Bioaugmentation of syntrophic acetate-oxidizing culture in biogas reactors exposed to increasing levels of ammonia. Appl. Environ. Microbiol. 78 (21), 7619–7625.
Whiteley, A.S., Thomson, B., Lueders, T., Manefield, M., 2007. RNA stable-isotope probing. Nat. Protoc. 2 (4), 838–844.
Wiegant, W.M., Zeeman, G., 1986. The mechanism of ammonia inhibition in the thermophilic digestion of livestock wastes. Agric. Wastes 16 (4), 243–253.
Worm, P., Fermoso, F.G., Lens, P.N., Plugge, C.M., 2009. Decreased activity of a propionate degrading community in a UASB reactor fed with synthetic medium without molybdenum, tungsten and selenium. Enzym. Microb. Technol. 45 (2), 139–145.
Yuan, Y., Conrad, R., Lu, Y., 2011. Transcriptional response of methanogen *mcrA* genes to oxygen exposure of rice field soil. Environ. Microbiol. Rep. 3 (3), 320–328.
Zamanzadeh, M., Parker, W.J., Verastegui, Y., Neufeld, J.D., 2013. Biokinetics and bacterial communities of propionate oxidizing bacteria in phased anaerobic sludge digestion systems. Water Res. 47 (4), 1558–1569.
Zhang, C., Yuan, Q., Lu, Y., 2014. Inhibitory effects of ammonia on methanogen *mcrA* transcripts in anaerobic digester sludge. FEMS Microbiol. Ecol. 87, 368–377.